

Search for the Standard Model Higgs Boson in the $H \rightarrow WW \rightarrow l\nu q'\bar{q}$ Decay Channel

V. M. Abazov,³⁵ B. Abbott,⁷² B. S. Acharya,²⁹ M. Adams,⁴⁸ T. Adams,⁴⁶ G. D. Alexeev,³⁵ G. Alkhazov,³⁹ A. Alton,^{60,*} G. Alverson,⁵⁹ G. A. Alves,² L. S. Ancu,³⁴ M. Aoki,⁴⁷ M. Arov,⁵⁷ A. Askew,⁴⁶ B. Åsman,⁴⁰ O. Atramentov,⁶⁴ C. Avila,⁸ J. BackusMayes,⁷⁹ F. Badaud,¹³ L. Bagby,⁴⁷ B. Baldin,⁴⁷ D. V. Bandurin,⁴⁶ S. Banerjee,²⁹ E. Barberis,⁵⁹ P. Baringer,⁵⁵ J. Barreto,³ J. F. Bartlett,⁴⁷ U. Bassler,¹⁸ V. Bazterra,⁴⁸ S. Beale,⁶ A. Bean,⁵⁵ M. Begalli,³ M. Begel,⁷⁰ C. Belanger-Champagne,⁴⁰ L. Bellantoni,⁴⁷ S. B. Beri,²⁷ G. Bernardi,¹⁷ R. Bernhard,²² I. Bertram,⁴¹ M. Besançon,¹⁸ R. Beuselinck,⁴² V. A. Bezzubov,³⁸ P. C. Bhat,⁴⁷ V. Bhatnagar,²⁷ G. Blazey,⁴⁹ S. Blessing,⁴⁶ K. Bloom,⁶³ A. Boehnlein,⁴⁷ D. Boline,⁶⁹ T. A. Bolton,⁵⁶ E. E. Boos,³⁷ G. Borissov,⁴¹ T. Bose,⁵⁸ A. Brandt,⁷⁵ O. Brandt,²³ R. Brock,⁶¹ G. Brooijmans,⁶⁷ A. Bross,⁴⁷ D. Brown,¹⁷ J. Brown,¹⁷ X. B. Bu,⁴⁷ M. Buehler,⁷⁸ V. Buescher,²⁴ V. Bunichev,³⁷ S. Burdin,^{41,†} T. H. Burnett,⁷⁹ C. P. Buszello,⁴⁰ B. Calpas,¹⁵ E. Camacho-Pérez,³² M. A. Carrasco-Lizarraga,⁵⁵ B. C. K. Casey,⁴⁷ H. Castilla-Valdez,³² S. Chakrabarti,⁶⁹ D. Chakraborty,⁴⁹ K. M. Chan,⁵³ A. Chandra,⁷⁷ G. Chen,⁵⁵ S. Chevalier-Théry,¹⁸ D. K. Cho,⁷⁴ S. W. Cho,³¹ S. Choi,³¹ B. Choudhary,²⁸ T. Christoudias,⁴² S. Cihangir,⁴⁷ D. Claes,⁶³ J. Clutter,⁵⁵ M. Cooke,⁴⁷ W. E. Cooper,⁴⁷ M. Corcoran,⁷⁷ F. Couderc,¹⁸ M.-C. Cousinou,¹⁵ A. Croc,¹⁸ D. Cutts,⁷⁴ A. Das,⁴⁴ G. Davies,⁴² K. De,⁷⁵ S. J. de Jong,³⁴ E. De La Cruz-Burelo,³² F. Déliot,¹⁸ M. Demarteau,⁴⁷ R. Demina,⁶⁸ D. Denisov,⁴⁷ S. P. Denisov,³⁸ S. Desai,⁴⁷ K. DeVaughan,⁶³ H. T. Diehl,⁴⁷ M. Diesburg,⁴⁷ A. Dominguez,⁶³ T. Dorland,⁷⁹ A. Dubey,²⁸ L. V. Dudko,³⁷ D. Duggan,⁶⁴ A. Duperrin,¹⁵ S. Dutt,²⁷ A. Dyshkant,⁴⁹ M. Eads,⁶³ D. Edmunds,⁶¹ J. Ellison,⁴⁵ V. D. Elvira,⁴⁷ Y. Enari,¹⁷ H. Evans,⁵¹ A. Evdokimov,⁷⁰ V. N. Evdokimov,³⁸ G. Facini,⁵⁹ T. Ferbel,⁶⁸ F. Fiedler,²⁴ F. Filthaut,³⁴ W. Fisher,⁶¹ H. E. Fisk,⁴⁷ M. Fortner,⁴⁹ H. Fox,⁴¹ S. Fuess,⁴⁷ T. Gadfort,⁷⁰ A. Garcia-Bellido,⁶⁸ V. Gavrilov,³⁶ P. Gay,¹³ W. Geist,¹⁹ W. Geng,^{15,61} D. Gerbaudo,⁶⁵ C. E. Gerber,⁴⁸ Y. Gershtein,⁶⁴ G. Ginther,^{47,68} G. Golovanov,³⁵ A. Goussiou,⁷⁹ P. D. Grannis,⁶⁹ S. Greder,¹⁹ H. Greenlee,⁴⁷ Z. D. Greenwood,⁵⁷ E. M. Gregores,⁴ G. Grenier,²⁰ Ph. Gris,¹³ J.-F. Grivaz,¹⁶ A. Grohsjean,¹⁸ S. Grünendahl,⁴⁷ M. W. Grünewald,³⁰ F. Guo,⁶⁹ G. Gutierrez,⁴⁷ P. Gutierrez,⁷² A. Haas,^{67,‡} S. Hagopian,⁴⁶ J. Haley,⁵⁹ L. Han,⁷ K. Harder,⁴³ A. Harel,⁶⁸ J. M. Hauptman,⁵⁴ J. Hays,⁴² T. Head,⁴³ T. Hebbeker,²¹ D. Hedin,⁴⁹ H. Hegab,⁷³ A. P. Heinson,⁴⁵ U. Heintz,⁷⁴ C. Hensel,²³ I. Heredia-De La Cruz,³² K. Herner,⁶⁰ M. D. Hildreth,⁵³ R. Hirosky,⁷⁸ T. Hoang,⁴⁶ J. D. Hobbs,⁶⁹ B. Hoeneisen,¹² M. Hohlfield,²⁴ S. Hossain,⁷² Z. Hubacek,^{10,18} N. Huske,¹⁷ V. Hynek,¹⁰ I. Iashvili,⁶⁶ R. Illingworth,⁴⁷ A. S. Ito,⁴⁷ S. Jabeen,⁷⁴ M. Jaffré,¹⁶ S. Jain,⁶⁶ D. Jamin,¹⁵ R. Jesik,⁴² K. Johns,⁴⁴ M. Johnson,⁴⁷ D. Johnston,⁶³ A. Jonckheere,⁴⁷ P. Jonsson,⁴² J. Joshi,²⁷ A. Juste,^{47,§} K. Kaadze,⁵⁶ E. Kajfasz,¹⁵ D. Karmanov,³⁷ P. A. Kasper,⁴⁷ I. Katsanos,⁶³ R. Kehoe,⁷⁶ S. Kermiche,¹⁵ N. Khalatyan,⁴⁷ A. Khanov,⁷³ A. Kharchilava,⁶⁶ Y. N. Kharzheev,³⁵ D. Khatidze,⁷⁴ M. H. Kirby,⁵⁰ J. M. Kohli,²⁷ A. V. Kozelov,³⁸ J. Kraus,⁶¹ A. Kumar,⁶⁶ A. Kupco,¹¹ T. Kurča,²⁰ V. A. Kuzmin,³⁷ J. Kvita,⁹ S. Lammers,⁵¹ G. Landsberg,⁷⁴ P. Lebrun,²⁰ H. S. Lee,³¹ S. W. Lee,⁵⁴ W. M. Lee,⁴⁷ J. Lellouch,¹⁷ L. Li,⁴⁵ Q. Z. Li,⁴⁷ S. M. Lietti,⁵ J. K. Lim,³¹ D. Lincoln,⁴⁷ J. Linnemann,⁶¹ V. V. Lipaev,³⁸ R. Lipton,⁴⁷ Y. Liu,⁷ Z. Liu,⁶ A. Lobodenko,³⁹ M. Lokajicek,¹¹ P. Love,⁴¹ H. J. Lubatti,⁷⁹ R. Luna-Garcia,^{32,||} A. L. Lyon,⁴⁷ A. K. A. Maciel,² D. Mackin,⁷⁷ R. Madar,¹⁸ R. Magaña-Villalba,³² S. Malik,⁶³ V. L. Malyshev,³⁵ Y. Maravin,⁵⁶ J. Martínez-Ortega,³² R. McCarthy,⁶⁹ C. L. McGivern,⁵⁵ M. M. Meijer,³⁴ A. Melnitchouk,⁶² D. Menezes,⁴⁹ P. G. Mercadante,⁴ M. Merkin,³⁷ A. Meyer,²¹ J. Meyer,²³ F. Miconi,¹⁹ N. K. Mondal,²⁹ G. S. Muanza,¹⁵ M. Mulhearn,⁷⁸ E. Nagy,¹⁵ M. Naimuddin,²⁸ M. Narain,⁷⁴ R. Nayyar,²⁸ H. A. Neal,⁶⁰ J. P. Negret,⁸ P. Neustroev,³⁹ S. F. Novaes,⁵ T. Nunnemann,²⁵ G. Obrant,³⁹ J. Orduna,³² N. Osman,⁴² J. Osta,⁵³ G. J. Otero y Garzón,¹ M. Owen,⁴³ M. Padilla,⁴⁵ M. Pangilinan,⁷⁴ N. Parashar,⁵² V. Parihar,⁷⁴ S. K. Park,³¹ J. Parsons,⁶⁷ R. Partridge,^{74,‡} N. Parua,⁵¹ A. Patwa,⁷⁰ B. Penning,⁴⁷ M. Perfilov,³⁷ K. Peters,⁴³ Y. Peters,⁴³ G. Petrillo,⁶⁸ P. Pétrouff,¹⁶ R. Piegaia,¹ J. Piper,⁶¹ M.-A. Pleier,⁷⁰ P. L. M. Podesta-Lerma,^{32,||} V. M. Podstavkov,⁴⁷ M.-E. Pol,² P. Polozov,³⁶ A. V. Popov,³⁸ M. Prewitt,⁷⁷ D. Price,⁵¹ S. Protopopescu,⁷⁰ J. Qian,⁶⁰ A. Quadt,²³ B. Quinn,⁶² M. S. Rangel,² K. Ranjan,²⁸ P. N. Ratoff,⁴¹ I. Razumov,³⁸ P. Renkel,⁷⁶ M. Rijssenbeek,⁶⁹ I. Ripp-Baudot,¹⁹ F. Rizatdinova,⁷³ M. Rominsky,⁴⁷ C. Royon,¹⁸ P. Rubinov,⁴⁷ R. Ruchti,⁵³ G. Safronov,³⁶ G. Sajot,¹⁴ A. Sánchez-Hernández,³² M. P. Sanders,²⁵ B. Sanghi,⁴⁷ A. S. Santos,⁵ G. Savage,⁴⁷ L. Sawyer,⁵⁷ T. Scanlon,⁴² R. D. Schamberger,⁶⁹ Y. Scheglov,³⁹ H. Schellman,⁵⁰ T. Schliephake,²⁶ S. Schlobohm,⁷⁹ C. Schwanenberger,⁴³ R. Schwienhorst,⁶¹ J. Sekaric,⁵⁵ H. Severini,⁷² E. Shabalina,²³ V. Shary,¹⁸ A. A. Shchukin,³⁸ R. K. Shivpuri,²⁸ V. Simak,¹⁰ V. Sirotenko,⁴⁷ P. Skubic,⁷² P. Slattery,⁶⁸ D. Smirnov,⁵³ K. J. Smith,⁶⁶ G. R. Snow,⁶³ J. Snow,⁷¹ S. Snyder,⁷⁰ S. Söldner-Rembold,⁴³ L. Sonnenschein,²¹ A. Sopczak,⁴¹ M. Sosebee,⁷⁵ K. Soustruznik,⁹ B. Spurlock,⁷⁵ J. Stark,¹⁴ V. Stolin,³⁶ D. A. Stoyanova,³⁸ M. Strauss,⁷² D. Strom,⁴⁸ L. Stutte,⁴⁷ L. Suter,⁴³ P. Svoisky,⁷² M. Takahashi,⁴³ A. Tanasijczuk,¹ W. Taylor,⁶ M. Titov,¹⁸ V. V. Tokmenin,³⁵ Y.-T. Tsai,⁶⁸ D. Tsybychev,⁶⁹ B. Tuchming,¹⁸ C. Tully,⁶⁵ P. M. Tuts,⁶⁷ L. Uvarov,³⁹ S. Uvarov,³⁹ S. Uzunyan,⁴⁹ R. Van Kooten,⁵¹ W. M. van Leeuwen,³³ N. Varelas,⁴⁸

E. W. Varnes,⁴⁴ I. A. Vasilyev,³⁸ P. Verdier,²⁰ L. S. Vertogradov,³⁵ M. Verzocchi,⁴⁷ M. Vesterinen,⁴³ D. Vilanova,¹⁸
 P. Vint,⁴² P. Vokac,¹⁰ H. D. Wahl,⁴⁶ M. H. L. S. Wang,⁶⁸ J. Warchol,⁵³ G. Watts,⁷⁹ M. Wayne,⁵³ M. Weber,^{47,**}
 L. Welty-Rieger,⁵⁰ A. White,⁷⁵ D. Wicke,²⁶ M. R. J. Williams,⁴¹ G. W. Wilson,⁵⁵ S. J. Wimpenny,⁴⁵ M. Wobisch,⁵⁷
 D. R. Wood,⁵⁹ T. R. Wyatt,⁴³ Y. Xie,⁴⁷ C. Xu,⁶⁰ S. Yacoob,⁵⁰ R. Yamada,⁴⁷ W.-C. Yang,⁴³ T. Yasuda,⁴⁷ Y. A. Yatsunenko,³⁵
 Z. Ye,⁴⁷ H. Yin,⁴⁷ K. Yip,⁷⁰ S. W. Youn,⁴⁷ J. Yu,⁷⁵ S. Zelitch,⁷⁸ T. Zhao,⁷⁹ B. Zhou,⁶⁰ J. Zhu,⁶⁰ M. Zielinski,⁶⁸
 D. Zieminska,⁵¹ and L. Zivkovic⁷⁴

(D0 Collaboration)

- ¹Universidad de Buenos Aires, Buenos Aires, Argentina
²LAFEX, Centro Brasileiro de Pesquisas Físicas, Rio de Janeiro, Brazil
³Universidade do Estado do Rio de Janeiro, Rio de Janeiro, Brazil
⁴Universidade Federal do ABC, Santo André, Brazil
⁵Instituto de Física Teórica, Universidade Estadual Paulista, São Paulo, Brazil
⁶Simon Fraser University, Vancouver, British Columbia, and York University, Toronto, Ontario, Canada
⁷University of Science and Technology of China, Hefei, People's Republic of China
⁸Universidad de los Andes, Bogotá, Colombia
⁹Charles University, Faculty of Mathematics and Physics, Center for Particle Physics, Prague, Czech Republic
¹⁰Czech Technical University in Prague, Prague, Czech Republic
¹¹Center for Particle Physics, Institute of Physics, Academy of Sciences of the Czech Republic, Prague, Czech Republic
¹²Universidad San Francisco de Quito, Quito, Ecuador
¹³LPC, Université Blaise Pascal, CNRS/IN2P3, Clermont, France
¹⁴LPSC, Université Joseph Fourier Grenoble 1, CNRS/IN2P3, Institut National Polytechnique de Grenoble, Grenoble, France
¹⁵CPPM, Aix-Marseille Université, CNRS/IN2P3, Marseille, France
¹⁶LAL, Université Paris-Sud, CNRS/IN2P3, Orsay, France
¹⁷LPNHE, Universités Paris VI and VII, CNRS/IN2P3, Paris, France
¹⁸CEA, Ifu, SPP, Saclay, France
¹⁹IPHC, Université de Strasbourg, CNRS/IN2P3, Strasbourg, France
²⁰IPNL, Université Lyon 1, CNRS/IN2P3, Villeurbanne, France and Université de Lyon, Lyon, France
²¹III. Physikalisches Institut A, RWTH Aachen University, Aachen, Germany
²²Physikalisches Institut, Universität Freiburg, Freiburg, Germany
²³II. Physikalisches Institut, Georg-August-Universität Göttingen, Göttingen, Germany
²⁴Institut für Physik, Universität Mainz, Mainz, Germany
²⁵Ludwig-Maximilians-Universität München, München, Germany
²⁶Fachbereich Physik, Bergische Universität Wuppertal, Wuppertal, Germany
²⁷Panjab University, Chandigarh, India
²⁸Delhi University, Delhi, India
²⁹Tata Institute of Fundamental Research, Mumbai, India
³⁰University College Dublin, Dublin, Ireland
³¹Korea Detector Laboratory, Korea University, Seoul, Korea
³²CINVESTAV, Mexico City, Mexico
³³FOM-Institute NIKHEF and University of Amsterdam/NIKHEF, Amsterdam, The Netherlands
³⁴Radboud University Nijmegen/NIKHEF, Nijmegen, The Netherlands
³⁵Joint Institute for Nuclear Research, Dubna, Russia
³⁶Institute for Theoretical and Experimental Physics, Moscow, Russia
³⁷Moscow State University, Moscow, Russia
³⁸Institute for High Energy Physics, Protvino, Russia
³⁹Petersburg Nuclear Physics Institute, St. Petersburg, Russia
⁴⁰Stockholm University, Stockholm and Uppsala University, Uppsala, Sweden
⁴¹Lancaster University, Lancaster LA1 4YB, United Kingdom
⁴²Imperial College London, London SW7 2AZ, United Kingdom
⁴³The University of Manchester, Manchester M13 9PL, United Kingdom
⁴⁴University of Arizona, Tucson, Arizona 85721, USA
⁴⁵University of California Riverside, Riverside, California 92521, USA
⁴⁶Florida State University, Tallahassee, Florida 32306, USA
⁴⁷Fermi National Accelerator Laboratory, Batavia, Illinois 60510, USA
⁴⁸University of Illinois at Chicago, Chicago, Illinois 60607, USA
⁴⁹Northern Illinois University, DeKalb, Illinois 60115, USA
⁵⁰Northwestern University, Evanston, Illinois 60208, USA

- ⁵¹Indiana University, Bloomington, Indiana 47405, USA
⁵²Purdue University Calumet, Hammond, Indiana 46323, USA
⁵³University of Notre Dame, Notre Dame, Indiana 46556, USA
⁵⁴Iowa State University, Ames, Iowa 50011, USA
⁵⁵University of Kansas, Lawrence, Kansas 66045, USA
⁵⁶Kansas State University, Manhattan, Kansas 66506, USA
⁵⁷Louisiana Tech University, Ruston, Louisiana 71272, USA
⁵⁸Boston University, Boston, Massachusetts 02215, USA
⁵⁹Northeastern University, Boston, Massachusetts 02115, USA
⁶⁰University of Michigan, Ann Arbor, Michigan 48109, USA
⁶¹Michigan State University, East Lansing, Michigan 48824, USA
⁶²University of Mississippi, University, Mississippi 38677, USA
⁶³University of Nebraska, Lincoln, Nebraska 68588, USA
⁶⁴Rutgers University, Piscataway, New Jersey 08855, USA
⁶⁵Princeton University, Princeton, New Jersey 08544, USA
⁶⁶State University of New York, Buffalo, New York 14260, USA
⁶⁷Columbia University, New York, New York 10027, USA
⁶⁸University of Rochester, Rochester, New York 14627, USA
⁶⁹State University of New York, Stony Brook, New York 11794, USA
⁷⁰Brookhaven National Laboratory, Upton, New York 11973, USA
⁷¹Langston University, Langston, Oklahoma 73050, USA
⁷²University of Oklahoma, Norman, Oklahoma 73019, USA
⁷³Oklahoma State University, Stillwater, Oklahoma 74078, USA
⁷⁴Brown University, Providence, Rhode Island 02912, USA
⁷⁵University of Texas, Arlington, Texas 76019, USA
⁷⁶Southern Methodist University, Dallas, Texas 75275, USA
⁷⁷Rice University, Houston, Texas 77005, USA
⁷⁸University of Virginia, Charlottesville, Virginia 22901, USA
⁷⁹University of Washington, Seattle, Washington 98195, USA
(Received 30 January 2011; published 28 April 2011)

We present a search for the standard model Higgs boson (H) in $p\bar{p}$ collisions at $\sqrt{s} = 1.96$ TeV in events containing a charged lepton (ℓ), missing transverse energy, and at least two jets, using 5.4 fb^{-1} of integrated luminosity recorded with the D0 detector at the Fermilab Tevatron Collider. This analysis is sensitive primarily to Higgs bosons produced through the fusion of two gluons or two electroweak bosons, with subsequent decay $H \rightarrow WW \rightarrow \ell\nu q'\bar{q}$, where ℓ is an electron or muon. The search is also sensitive to contributions from other production channels, such as $WH \rightarrow \ell\nu b\bar{b}$. In the absence of a signal, we set limits at the 95% C.L. on the cross section for H production $\sigma(p\bar{p} \rightarrow H + X)$ in these final states. For a mass of $M_H = 160$ GeV, the limit is a factor of 3.9 larger than the cross section in the standard model and consistent with an *a priori* expected sensitivity of 5.0.

DOI: 10.1103/PhysRevLett.106.171802

PACS numbers: 14.80.Bn, 13.85.Rm

The Higgs mechanism [1–4] accommodates the observed breaking of electroweak symmetry in the standard model (SM). In addition to generating masses for the electroweak W and Z bosons, as well as for fermions, the theory predicts a scalar Higgs boson (H) with well-determined couplings but unknown mass (M_H). Confirmation of the existence and properties of the H boson would be a key step in elucidating the origins of electroweak symmetry breaking. For a Higgs boson with mass $M_H \gtrsim 135$ GeV, the dominant decay mode is $H \rightarrow W^+W^-$, where at least one W boson must be virtual when $M_H < 2M_W$. Previous searches [5–7] for this process were based on events with two charged leptons (ℓ) and large missing transverse energy (E_T) from the decay $H \rightarrow W^+W^- \rightarrow \bar{\ell}\nu\ell'\bar{\nu}'$ ($\ell = e, \mu$). This Letter presents

the first search for production of Higgs bosons with subsequent decay to WW having only one charged lepton in the final state. The data correspond to 5.4 fb^{-1} of integrated luminosity from $p\bar{p}$ collisions at $\sqrt{s} = 1.96$ TeV recorded with the D0 detector at the Fermilab Tevatron Collider. The largest SM contributions to the inclusive cross section for producing H bosons in $p\bar{p}$ collisions are from mechanisms involving the fusion of two gluons or two weak vector bosons into an H boson, and associated production of H and a weak vector boson ($V = W$ or Z). In the following we will not distinguish between particles and antiparticles. The most striking signatures from $H \rightarrow VV$ decays are the all-leptonic 4ℓ and $2\ell 2\nu$ final states, but these account for only $\approx 5\%$ of all decays. Final states containing a single charged lepton have larger

backgrounds, but their branching fractions are a factor of ≈ 6 larger than for the all-leptonic modes.

A recent calculation of the differential width for $H \rightarrow WW \rightarrow \ell\nu q'q$ decays [8] supports the importance of these mixed modes for characterizing a potential SM Higgs-boson signal. Our analysis is most sensitive to final-state topologies with a single charged lepton, two or more jets, and E_T arising from $H \rightarrow WW \rightarrow \ell\nu q'q$ decays. For $M_H \lesssim 140$ GeV, significant sensitivity is gained from the $WH \rightarrow \ell\nu bb$ channel, where we do not attempt to identify the b quark flavor. Smaller contributions from $H \rightarrow ZZ \rightarrow \ell\ell qq$, where ℓ represents an unidentified lepton and $H \rightarrow WW \rightarrow \tau\nu q'q$ with $\tau \rightarrow \ell\nu\nu$, are also included. For $M_H \geq 160$ GeV, by assuming that the observed E_T is due to the neutrino from the decay of a W boson, it is possible to reconstruct the longitudinal momentum of the neutrino (p_z^ν) up to a twofold ambiguity and thereby extract M_H from the WW decay [9]. We choose the solution with smallest $|\text{Re}(p_z^\nu)|$ to calculate M_H , resulting in the correct choice for $\approx 70\%$ of signal events. The primary backgrounds are from $V + \text{jets}$, top quark and diboson production, and multijet (MJ) events containing a lepton or leptonlike signature, with E_T generally arising from the mismeasurement of jet energies.

The D0 detector [10] consists of tracking, calorimetric, and muon subsystems. Charged particle tracks are reconstructed by using silicon microstrip detectors and a scintillating fiber tracker, within a 2 T solenoid. Three uranium-liquid-argon calorimeters measure particle energies that are reconstructed into hadronic jets using an iterative midpoint cone algorithm with a cone radius of 0.5 [11]. Electrons and muons are identified through association of charged particle tracks with clusters in the electromagnetic sections of the calorimeters or with hits in the muon detector, respectively. We obtain the E_T from a vector sum of transverse components of calorimeter energy depositions and correct it for identified muons. Jet energies are calibrated by using transverse momentum balance in photon + jet events [12], and the correction is propagated to the E_T . The data are recorded by using triggers designed to select single electrons or muons and combinations of an electron and jets. After imposing data quality requirements, the total integrated luminosity is 5.4 fb^{-1} [13], where the first 1.1 fb^{-1} , run IIa, precedes an upgrade to the silicon microstrip and trigger systems. The remaining 4.3 fb^{-1} is denoted as run IIb. The four data sets, e or μ for

the two run epochs, are analyzed separately and combined in the final result.

Background contributions from most SM processes are simulated by using Monte Carlo (MC) generators, with normalizations constrained by the data, whereas the multi-jet background is fully estimated from the data. The dominant background is from $V + \text{jets}$ processes, which are generated with ALPGEN [14]. The transverse momentum (p_T) spectrum of the Z boson in MC is reweighted to match that observed in the data [15]. The p_T spectrum of the W boson is reweighted by using the same dependence but corrected for differences between the p_T spectra of Z and W bosons predicted in next-to-next-to-leading order QCD [16]. Backgrounds from $t\bar{t}$ and electroweak single-top quark production are simulated by using the ALPGEN and COMPHEP [17] generators, respectively. Vector-boson pair production and H boson signals are generated with PYTHIA [18]. All these simulations use CTEQ6L1 parton distribution functions [19]. Both ALPGEN and COMPHEP samples are interfaced with PYTHIA to model parton evolution and hadronization.

Relative normalizations for the various $V + \text{jets}$ processes are obtained from calculations of cross sections at next-to-leading order using MCFM [20], while the absolute normalization for the total $V + \text{jets}$ background is constrained through a comparison to the data, following the subtraction of other background sources. This increases the normalization for $V + \text{jets}$ background by about 2%, compared with the expectation from ALPGEN normalized by using total cross sections calculated at next-to-next-to-leading order [21] with the MRST2004 next-to-next-to-leading order parton distribution functions [22]. Cross sections for other SM backgrounds are taken from Ref. [23] or calculated with MCFM, and those for signal are taken from Ref. [24]. The p_T spectra for diboson events in background are corrected to match those of the MC@NLO generator [25]. The p_T spectra from the contribution of gluon fusion to the H boson signal, as generated in PYTHIA, are modified to match those obtained from SHERPA [26].

Signal and background events from MC are passed through a full GEANT3-based simulation [27] of detector response and then processed with the same reconstruction program as used for the data. Events from randomly selected beam crossings, corresponding to the same instantaneous luminosity profile as the data, are overlaid on the simulated events to model detector noise and contributions

TABLE I. Number of signal and background events expected after selection requirements. The signal sources include gluon-gluon and vector-boson fusion and associated production WH . The three numbers quoted for the signals correspond to $M_H = 130, 160,$ and 190 GeV. For backgrounds, “Top” includes pair and single-top quark production and “VV” includes all nonsignal diboson processes. The overall background normalization is fixed to the data by adjusting the $V + \text{jets}$ cross sections.

Channel	$gg \rightarrow H$	$qq \rightarrow qqH$	WH	$V + \text{jets}$	Multijet	Top	VV	Total background	Data
Electron	11.2 46.3 27.8	2.1 6.4 4.2	7.2 0 0	52 158	11 453	2433	1584	67 627	67 627
Muon	9.5 34.7 20.4	1.5 4.4 2.9	5.7 0 0	47 970	2720	1598	1273	53 562	53 562

from the presence of additional $p\bar{p}$ interactions. Parameterizations of trigger efficiency for leptons are determined by using $Z \rightarrow \ell\ell$ decays [28]. Any remaining differences between the data and simulation in the reconstruction of electrons, muons, and jets are adjusted in simulated events to match those observed in the data, and these corrections are also propagated to the E_T .

Events are selected to contain candidates for $W \rightarrow \ell\nu$ decay by requiring $E_T > 15$ GeV and the presence of a lepton with $p_T > 15$ GeV that is isolated relative to jets, namely, located outside jet cones, $\Delta R(\ell, j) > 0.5$, with $(\Delta R)^2 = (\phi^\ell - \phi^j)^2 + (\eta^\ell - \eta^j)^2$, where ϕ^x and η^x are, respectively, the azimuth and pseudorapidity [29] of object x . The position of the $p\bar{p}$ interaction vertex (PV) along the beam direction (z_{PV}) is required to be reconstructed within the longitudinal acceptance of the silicon microstrip, $|z_{PV}| < 60$ cm. The lepton is required to originate from the PV and to pass more restrictive isolation criteria based on tracking information and energy deposited near its trajectory in the calorimeter. Electrons must also satisfy criteria on the spatial distribution of the shower, and timing information is used to reject the cosmic ray background in events with muons. All lepton selections are described in Ref. [30], except that this analysis requires both the scalar sum of track p_T and calorimeter energy in the vicinity of the muon to be less than 2.5 GeV. Electrons and muons are required to be located within $|\eta_{\text{det}}| < 1.1$ and < 1.6 , respectively, where η_{det} is the pseudorapidity assuming the object originates from the center of the detector. To reduce background from $Z \rightarrow \ell\ell$, top quark, and diboson events, and to assure selected events do not overlap those used in $WW \rightarrow \ell\nu\ell'\nu'$ analysis channels, we veto any event containing an additional lepton satisfying less stringent identification criteria. We also require at least two jets with $|\eta^j| < 2.5$ and $p_T > 20$ GeV that contain associated tracks originating from the PV. The jet p_T requirement is 23 GeV when the second-leading jet (ordered in p_T) has $0.8 < |\eta_{\text{det}}| < 1.5$ [10]. The two leading jets are used to reconstruct the W boson decaying to $q'q$. To suppress background from MJ events [31], we require events to have $M_T^W(\text{GeV}) > (40 - 0.5)E_T$, where M_T^W is the transverse mass [32] of the W boson candidate.

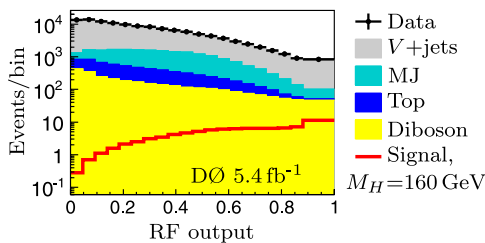


FIG. 1 (color online). The output of RF discriminants for the data, different backgrounds, and signal for $M_H = 160$ GeV for the combined data sets.

To estimate the MJ background, we use data samples orthogonal to our signal sample. For the electron channel, we form a “loose” category for which the selection on a likelihood discriminant used to select a “tight” electron, based on calorimeter and track variables [31], is reversed. Following the method of Ref. [33], the MJ background is evaluated from independently determined probabilities for loose electrons or jets to pass the tight signal selections. For the muon channel, we reverse requirements on muon isolation in both the tracking detectors and calorimeters and subtract contributions arising from SM processes containing a true muon from W or Z decay. The normalization is obtained from fits to both the $V + \text{jets}$ and MJ contributions using observed distributions of p_T^μ and E_T . Event yields in the data and those expected for the signal and background are shown in Table I.

We use a random forest (RF) of 50 decision trees to separate the signal from the background [34,35]. Each decision tree is trained on a randomly selected collection of signal and background MC events and also MJ events from the data. The decision trees examine a random set of about 30 discriminating variables formed from particle four-vectors, angles between objects, and combinations of kinematic variables such as reconstructed masses and event shapes. An RF is trained separately for each data set, by using signal hypotheses $115 < M_H < 200$ GeV in steps of 5 GeV. The strongest discriminants in each RF vary with M_H . The dominant variables are, for $M_H < 2M_W$, the three-body mass (ℓjj); for $M_H \approx 2M_W$, variables involving relative angles between objects; and for $M_H > 2M_W$, variables related to the decay of a boosted W boson. The outputs of the final RF discriminants for the four data sets combined, background, and signal for $M_H = 160$ GeV are shown in Fig. 1. Agreement is observed with expectations from the SM background, and the RF-output distributions are therefore used to set upper limits on the cross section for SM Higgs production.

Systematic uncertainties affect the normalizations and distributions of the final discriminants and are therefore included in the determination of limits. These arise from a

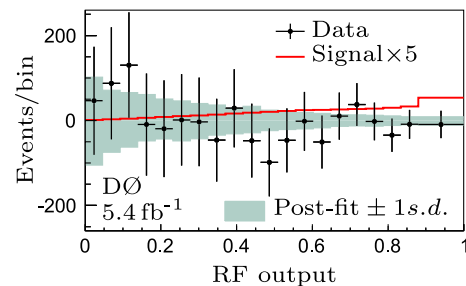


FIG. 2 (color online). The combined background-subtracted data and 1 standard deviation (s.d.) uncertainty on the total background after applying constraints on systematic uncertainties by fitting to the data. The expected SM Higgs signal for $M_H = 160$ GeV, shown by the line, is scaled up by a factor of 5.

TABLE II. Ratios of the observed and expected exclusion limits relative to the SM production cross section for $\sigma(p\bar{p} \rightarrow H + X)$ multiplied by the branching fraction for $H + X \rightarrow \ell + \ell/\nu + qq$ at the 95% C.L. as a function of M_H .

M_H (GeV)	115	120	125	130	135	140	145	150	155	160	165	170	175	180	185	190	195	200
Observed	28.5	20.4	32.8	36.6	33.0	33.7	23.1	17.1	8.3	3.9	5.2	5.6	8.2	7.1	12.0	10.6	10.0	10.4
Expected	19.5	23.4	26.4	28.4	25.7	19.7	13.7	10.4	8.0	5.0	5.1	5.9	6.7	8.0	9.6	10.7	11.2	12.1

variety of sources, and their impact is assessed by changing each input discriminant to the RF by ± 1 standard deviation. The most significant uncertainties affecting the normalizations are from calibration of jet energies (0.7–6)%, jet resolution (0.5–3)%, jet reconstruction efficiency (0.5–4)%, lepton identification and modeling of the trigger (4%), estimation of multijet background (6.5–26)%, and integrated luminosity (6.1%). Theoretical uncertainties on cross sections for backgrounds are taken from Refs. [20,23]. The uncertainties on cross sections for the signal are taken from Ref. [24]. Because the overall cross section for $V + \text{jets}$ production is constrained by the data, the uncertainty on its normalization is anticorrelated with the MJ background. The impact of theoretical uncertainties on distributions of the final discriminants is assessed by varying a common renormalization and factorization scale, by comparing ALPGEN interfaced with HERWIG [36] to ALPGEN interfaced with PYTHIA for $V + \text{jets}$ samples, and by varying the parton distribution function parameters using the prescription of Ref. [19] for all MC samples.

Upper limits on the production cross section multiplied by branching fractions are determined by using the modified frequentist CL_S approach [37]. A test statistic based on the logarithm of the ratio of likelihoods (LLR) [37] for the data to represent signal + background and background-only hypotheses is summed over all bins of the final discriminant in each data set. To minimize degradation in sensitivity, scaling factors for the systematic uncertainties are fitted to the data by maximizing a likelihood function

for both the signal + background and background-only hypotheses, with the systematic uncertainties constrained through Gaussian priors on their probabilities [38]. Correlations among systematic uncertainties in the signal and background are taken into account in extracting the final results. Figure 2 shows the combined background-subtracted data and the uncertainties on the RF discriminant after they are fitted to the data.

The resulting limits on standard model Higgs-boson production are given in Table II. The LLR_{OBS} values shown in Fig. 3 as functions of M_H are within ~ 1.5 standard deviations of the expected median for LLR_B , the background-only hypothesis, as calculated from statistical fluctuations and systematic uncertainties.

In conclusion, we have determined the first limits on standard model Higgs-boson production by examining decays of the Higgs boson to two vector bosons, one of which decays leptonically and the other into a pair of quarks. For $M_H = 160$ GeV, the observed and expected 95% C.L. upper limits on the combined cross section for Higgs production, multiplied by the branching fraction for $H + X \rightarrow \ell + \ell/\nu + qq$, are factors of 3.9 and 5.0 larger than the SM cross section, respectively.

Supplemental material, including a list of variables used in the RF, samples of input distributions, and a table of systematic uncertainties, is available [39].

We thank the staffs at Fermilab and collaborating institutions and acknowledge support from the DOE and NSF (USA); CEA and CNRS/IN2P3 (France); FASI, Rosatom, and RFBR (Russia); CNPq, FAPERJ, FAPESP, and FUNDUNESP (Brazil); DAE and DST (India); Colciencias (Colombia); CONACyT (Mexico); KRF and KOSEF (Korea); CONICET and UBACyT (Argentina); FOM (The Netherlands); STFC and the Royal Society (United Kingdom); MSMT and GACR (Czech Republic); CRC Program and NSERC (Canada); BMBF and DFG (Germany); SFI (Ireland); The Swedish Research Council (Sweden); and CAS and CNSF (China).

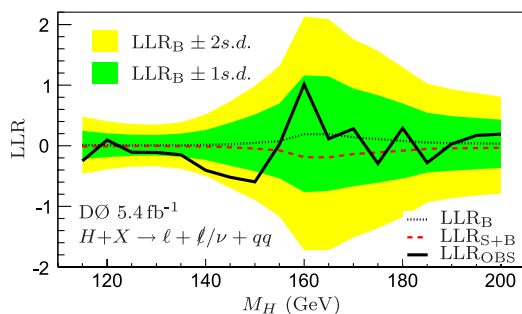


FIG. 3 (color online). The observed LLRs for the combined data are given by the solid line. Expected LLRs for the background-only and signal + background hypotheses are shown as dots and dashes, respectively, and the dark and light-shaded areas correspond to 1 and 2 s.d. around the expected LLR for the background-only hypothesis. Negative values of LLR_{OBS} represent signal-like fluctuations in the data.

*Visitor from Augustana College, Sioux Falls, SD, USA.

†Visitor from The University of Liverpool, Liverpool, United Kingdom.

‡Visitor from SLAC, Menlo Park, CA, USA.

§Visitor from ICREA/IFAE, Barcelona, Spain.

||Visitor from Centro de Investigacion en Computacion—IPN, Mexico City, Mexico.

- [¶]Visitor from ECFM, Universidad Autonoma de Sinaloa, Culiacán, Mexico.
- ^{**}Visitor from Universität Bern, Bern, Switzerland.
- [1] F. Englert and R. Brout, *Phys. Rev. Lett.* **13**, 321 (1964).
- [2] P. W. Higgs, *Phys. Rev. Lett.* **13**, 508 (1964).
- [3] G. S. Guralnik, C. R. Hagen, and T. W. B. Kibble, *Phys. Rev. Lett.* **13**, 585 (1964).
- [4] P. W. Higgs, *Phys. Rev.* **145**, 1156 (1966).
- [5] V. M. Abazov *et al.* (D0 Collaboration), *Phys. Rev. Lett.* **104**, 061804 (2010).
- [6] T. Aaltonen *et al.* (CDF Collaboration), *Phys. Rev. Lett.* **104**, 061803 (2010).
- [7] T. Aaltonen *et al.* (CDF and D0 Collaborations), *Phys. Rev. Lett.* **104**, 061802 (2010).
- [8] B. Dobrescu and J. Lykken, *J. High Energy Phys.* **04** (2010) 083.
- [9] J. F. Gunion and M. Soldate, *Phys. Rev. D* **34**, 826 (1986).
- [10] V. M. Abazov *et al.* (D0 Collaboration), *Nucl. Instrum. Methods Phys. Res., Sect. A* **565**, 463 (2006); M. Abolins *et al.*, *Nucl. Instrum. Methods Phys. Res., Sect. A* **584**, 75 (2008); R. Angstadt *et al.*, *Nucl. Instrum. Methods Phys. Res., Sect. A* **622**, 298 (2010).
- [11] G. C. Blazey *et al.*, arXiv:hep-ex/0005012.
- [12] V. M. Abazov *et al.* (D0 Collaboration), *Phys. Rev. Lett.* **101**, 062001 (2008).
- [13] T. Andeen *et al.*, Fermilab Report No. FERMILAB-TM-2365, 2007.
- [14] M. L. Mangano *et al.*, *J. High Energy Phys.* **07** (2003) 001; version 2.11 was used.
- [15] V. M. Abazov *et al.* (D0 Collaboration), *Phys. Rev. Lett.* **100**, 102002 (2008).
- [16] K. Melnikov and F. Petriello, *Phys. Rev. D* **74**, 114017 (2006).
- [17] E. Boos *et al.* (CompHEP Collaboration), *Nucl. Instrum. Methods Phys. Res., Sect. A* **534**, 250 (2004).
- [18] T. Sjöstrand, S. Mrenna, and P. Skands, *J. High Energy Phys.* **05** (2006) 026; version 6.409 with TUNE A was used.
- [19] J. Pumplin *et al.*, *J. High Energy Phys.* **07** (2002) 012; D. Stump *et al.*, *J. High Energy Phys.* **10** (2003) 046.
- [20] J. M. Campbell and R. K. Ellis, *Phys. Rev. D* **65**, 113007 (2002).
- [21] R. Hamberg, W. L. van Neerven, and W. B. Kilgore, *Nucl. Phys.* **B359**, 343 (1991); **B644**, 403(E) (2002).
- [22] A. D. Martin, R. G. Roberts, W. J. Stirling, and R. S. Thorne, *Phys. Lett. B* **604**, 61 (2004).
- [23] M. Cacciari *et al.*, *J. High Energy Phys.* **04** (2004) 068; N. Kidonakis and R. Vogt, *Phys. Rev. D* **68**, 114014 (2003); N. Kidonakis, *Phys. Rev. D* **74**, 114012 (2006).
- [24] D. de Florian and M. Grazzini, *Phys. Lett. B* **674**, 291 (2009); C. Anastasiou, R. Boughezal, and F. Petriello, *J. High Energy Phys.* **04** (2009) 003; E. L. Berger and J. Campbell, *Phys. Rev. D* **70**, 073011 (2004); T. Hahn *et al.*, arXiv:hep-ph/0607308; M. L. Ciccolini, S. Dittmaier, and M. Krämer, *Phys. Rev. D* **68**, 073003 (2003); O. Brein, A. Djouadi, and R. Harlander, *Phys. Lett. B* **579**, 149 (2004); J. Baglio and A. Djouadi, *J. High Energy Phys.* **10** (2010) 064; A. Djouadi, J. Kalinowski, and M. Spira, *Comput. Phys. Commun.* **108**, 56 (1998).
- [25] S. Frixione and B. R. Webber, *J. High Energy Phys.* **06** (2002) 029.
- [26] T. Gleisberg *et al.*, *J. High Energy Phys.* **02** (2004) 056.
- [27] R. Brun and F. Carminati, CERN Program Library Long Writeup W5013, 1993 (unpublished).
- [28] V. M. Abazov *et al.* (D0 Collaboration), *Phys. Rev. D* **76**, 012004 (2007).
- [29] The pseudorapidity is defined as $\eta = -\ln[\tan(\theta/2)]$, where θ is the polar angle with respect to the proton beam direction.
- [30] V. M. Abazov *et al.* (D0 Collaboration), *Phys. Rev. D* **78**, 012005 (2008).
- [31] V. M. Abazov *et al.* (D0 Collaboration), *Phys. Rev. D* **75**, 092007 (2007).
- [32] V. M. Abazov *et al.* (D0 Collaboration), *Phys. Rev. Lett.* **103**, 141801 (2009).
- [33] V. M. Abazov *et al.* (D0 Collaboration), *Phys. Rev. D* **74**, 112004 (2006).
- [34] L. Breiman, *Mach. Learn.* **45**, 5 (2001).
- [35] I. Narsky, arXiv:physics/0507143; arXiv:physics/0507157.
- [36] G. Corcella *et al.*, *J. High Energy Phys.* **01** (2001) 010.
- [37] T. Junk, *Nucl. Instrum. Methods Phys. Res., Sect. A* **434**, 435 (1999); A. Read, *J. Phys. G* **28**, 2693 (2002).
- [38] W. Fisher, Fermilab, FERMILAB-TM-2386-E.
- [39] See supplemental material at <http://link.aps.org/supplemental/10.1103/PhysRevLett.106.171802> for additional details.